A FAMILY OF ALGORITHMS FOR BLIND EQUALIZATION OF QAM SIGNALS

João Mendes Filho, Magno T. M. Silva, and Maria D. Miranda

Escola Politécnica, University of São Paulo, São Paulo, SP, Brazil
E-mails: jmendes@lps.usp.br, magno@lps.usp.br, maria.miranda@poli.usp.br

ABSTRACT

We propose blind equalization algorithms that perform similarly to supervised ones, independently of the QAM order. They converge approximately to the Wiener solution, which generally provides a relatively low misadjustment. Besides presenting strategies to speed up their convergences, we provide sufficient conditions for the stability of the symbol-based decision algorithm, which is an extension of the decision-directed algorithm. Their behaviors are illustrated through simulation results.

Index Terms— Blind equalization, adaptive equalizers, QAM, constant modulus algorithm, decision-directed equalizer.

1. INTRODUCTION

High-order quadrature amplitude modulation (QAM) signalling is widely employed in digital communications systems in order to use the available bandwidth in an efficient manner [1]. This efficient use of bandwidth can be improved with blind equalizers, which play an important role to remove the intersymbol interference introduced by dispersive channels. The constant modulus algorithm (CMA) is the most popular for the adaptation of finite impulse response (FIR) equalizers due to its low computational cost. However, it has some drawbacks like the impossibility of solving phase ambiguities introduced by the channel and a relatively large misadjustment when used to recover nonconstant modulus signals, as is the case of high-order QAM signals (see, e.g., [2] and the references therein). Additionally, CMA can only achieve a zero steady-state mean-square error for constant modulus signals in a stationary and noiseless environment, and assuming a fractionally spaced equalizer (see, e.g., [3]).

The multimodulus algorithm (MMA) was proposed to solve the phase ambiguity issue through the minimization of the dispersion of the real and imaginary parts of the equalizer output separately. Although MMA provides better convergence for high-order QAM signals than that of CMA, it still exhibits a large misadjustment in the steady-state [4, 5]. In order to reduce the misadjustment exhibited by CMA and MMA in the equalization of QAM signals, many algorithms have been proposed in the literature (see, e.g., [6, 7, 8] and their references). In general, these algorithms achieve a steady-state misadjustment lower than that of MMA for QAM signals, but which is still relatively large when compared to the misadjustment obtained in the equalization of constant modulus signals with MMA. Furthermore, only few results have been shown for high-order QAM (more than 256 symbols).

In this paper, we propose a family of blind algorithms for equalization of low and high-order QAM signals that: (i) allows simultaneous recovery of the modulus and phase of the signal; (ii) has an error equal to zero when the equalizer output coincides with the transmitted signal; (iii) treats nonconstant modulus constellations as constant modulus ones, converging approximately to the Wiener solution, which generally provides a relatively low misadjustment; and (iv) presents faster convergence than existing blind multimodulus-type algorithms for equalization of QAM signals. With these properties, blind equalization algorithms tend to perform similarly to supervised ones, independently of the QAM order. We consider square QAM constellations throughout the paper. However, the proposed algorithms can be extended straightforwardly to non-square QAM constellations.

This work was partly supported by CAPES (scholarship of the institutional quota), CNPq under Grant 302633/2008-1, and FAPESP under Grant 2008/00773-1.

2. PROBLEM FORMULATION

The transmitted signal $a(n)$ is assumed independent, identically distributed, and non Gaussian. The channel is modeled by an FIR filter with impulse response vector $\mathbf{h}^T = [h_0\, h_1\, \cdots\, h_{K-1}]$ and additive white Gaussian noise (AWGN), where $(\cdot)^T$ indicates transposition. We assume an M-tap FIR equalizer, with input regressor vector $\mathbf{u}(n)$ and output $y(n) = \mathbf{u}^T(n)\mathbf{w}(n-1) = y_{\mathrm{R}}(n) + jy_{\mathrm{I}}(n)$, where $\mathbf{w}(n-1)$ is the equalizer weight vector and $y_{\mathrm{R}}(n)$ and $y_{\mathrm{I}}(n)$ are the real and imaginary parts of $y(n)$, respectively. The equalizer must mitigate the intersymbol interference and recover a delayed version of the signal $a(n) = a_{\mathrm{R}}(n) + ja_{\mathrm{I}}(n)$, obtaining the estimate $\hat{a}(n)$ at the output of the decision device. We focus on the following class of blind algorithms

$$\mathbf{w}(n) = \mathbf{w}(n-1) + \rho(n)e(n)\mathbf{u}^*(n), \tag{1}$$

where $\rho(n)$ is a step-size, $e(n)$ is the estimation error, and $(\cdot)^*$ stands for the complex-conjugate. Many blind equalization algorithms can be written as in (1), by proper choices of $\rho(n)$ and $e(n)$ [9]. In particular, we are interested in normalized algorithms, where $\rho(n) = \tilde{\mu}/(\delta + \|\mathbf{u}(n)\|^2)$, $\tilde{\mu}$ is a step-size, δ is a regularization factor, and $\|\cdot\|$ represents the Euclidean norm.

3. ERROR FUNCTIONS

In the multimodulus algorithm, the estimation error $e(n)$ is defined in terms of its real and imaginary parts separately, i.e,

$$e_{\mathrm{MMA}}(n) = [r - y_{\mathrm{R}}^2(n)]y_{\mathrm{R}}(n) + j[r - y_{\mathrm{I}}^2(n)]y_{\mathrm{I}}(n), \tag{2}$$

where $r = \mathrm{E}\{a_{\mathrm{R}}^4(n)\}/\mathrm{E}\{a_{\mathrm{R}}^2(n)\} = \mathrm{E}\{a_{\mathrm{I}}^4(n)\}/\mathrm{E}\{a_{\mathrm{I}}^2(n)\}$ and $\mathrm{E}\{\cdot\}$ is the expectation operator [4]. Fig. 1 shows the real part of the MMA error, denoted by $e_{\mathrm{MMA,R}}(n)$, as a function of $y_{\mathrm{R}}(n)$, assuming a constant (4-QAM) and a nonconstant (16-QAM) modulus signal (the figure for the imaginary counterpart is identical). For both signals, the real part of the MMA error is equal to zero when $y_{\mathrm{R}}^2(n)$ is null or when $y_{\mathrm{R}}^2(n)$ is equal to the dispersion constant r. For 4-QAM, $r = 1$ and $e_{\mathrm{MMA,R}}(n) = 0$ when the equalizer output is equal to the coordinates of the constellation symbols, i.e., $y_{\mathrm{R}}(n) = \pm 1$. This behavior does not occur for 16-QAM, since $r = 8.2$ and $|e_{\mathrm{MMA,R}}(n)| = 7.2$ and $|e_{\mathrm{MMA,R}}(n)| = 2.4$ for $y_{\mathrm{R}}(n) = \pm 1$ and $y_{\mathrm{R}}(n) = \pm 3$, respectively.

To improve the performance of CMA for nonconstant modulus signals, the radius-directed equalization (RDE) algorithm was proposed in [6]. While CMA uses a single dispersion constant, RDE uses multiple dispersion constants (consequently multiple radii), being the complex plane divided into annular decision regions chosen in an *adhoc* manner.

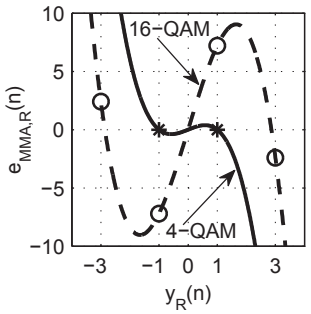

Fig. 1. Real part of the MMA error as a function of $y_{\rm R}(n)$ for 4-QAM and 16-QAM. The errors at the constellation symbol coordinates are indicated by $*$ (4-QAM) and $\circ$ (16-QAM).

Although the RDE error is smaller than that of CMA, the higher the QAM order, the smaller the distance among radii, and the worse the performance of the algorithm [6, 10]. Therefore, it can present slow convergence and high symbol error rates, which become unacceptable for low signal-to-noise ratios.

Considering a version of RDE in conjunction with MMA, we can observe that the distance between radii become evenly spaced, which implies a uniform behavior independently of the QAM order. Such version is termed hereinafter multimodulus radius-directed (MRD) algorithm and its estimation error is defined as

$$e_{\rm MRD}(n) = \big[\hat{a}_{\rm R}^2(n) - y_{\rm R}^2(n)\big]\, y_{\rm R}(n) + j\big[\hat{a}_{\rm I}^2(n) - y_{\rm I}^2(n)\big]\, y_{\rm I}(n), \quad (3)$$

where $\hat{a}_{\rm R}(n)$ (resp., $\hat{a}_{\rm I}(n)$) is the nearest real (resp., imaginary) part of the constellation symbol for $y_{\rm R}(n)$ (resp., $y_{\rm I}(n)$). To give further insight about this error, Fig. 2-(a) shows $e_{\rm MRD,R}(n)$ as a function of $y_{\rm R}(n)$ for 64-QAM (solid curve). The four dashed curves represent the error $e_{\rm MMA,R}(n)$ as a function of $y_{\rm R}(n)$ for a 4-QAM constellation with different scale factors. These factors are associated with the 4-QAM constellation symbols, i.e., $k\{\pm 1 \pm j\}, k = 1, 3, 5, 7$. The MRD error for 64-QAM coincides in intervals with the MMA error for the scaled 4-QAM constellations. For instance, we can observe from the figure that in the interval $4 < y_{\rm R}(n) < 6$, both the errors $e_{\rm MRD,R}(n)$ and $e_{\rm MMA,R}(n)$ with $k = 5$ are identical. The same occurs for the other values of the scale factor k. It is important to notice that the MRD error is zero when the equalizer output is equal to the symbol of the constellation, maintaining the same characteristic of the RDE error. Furthermore, since MRD uses multiple radii, the envelope of the solid curve in Fig. 2-(a) grows exponentially with the magnitude of $y_{\rm R}(n)$. This growing is related to the position of the symbol estimate and consequently to the scale factor k. Although the envelope is fundamental to the recovery of the transmitted symbols, its exponential growing can cause degradation in the performance of the algorithm, which becomes worse for high order QAM signals (higher than 256 symbols).

Based on the MRD error, we introduce now a symbol-based decision (SBD) algorithm, which is an extension of the decision-directed algorithm for equalization of QAM signals. We can observe that the MRD error (solid curve of Fig. 2-(a)) approaches to a straight line in every interval of $y_{\rm R}(n)$ between two abrupt changes, as in the decision-directed algorithm [9]. This behavior suggests the error shown in Fig. 2-(b) as a function of $y_{\rm R}(n)$ for a 64-QAM constellation. A general expression for this error is given by

$$e_{\rm SBD}(n) = |\hat{a}_{\rm R}(n)|\,[\hat{a}_{\rm R}(n) - y_{\rm R}(n)] + j|\hat{a}_{\rm I}(n)|\,[\hat{a}_{\rm I}(n) - y_{\rm I}(n)]. \quad (4)$$

It is relevant to notice that $|\hat{a}_{\rm R}(n)|$ and $|\hat{a}_{\rm I}(n)|$ create an envelope in the SBD error, which is essential to the recovery of the transmitted symbols. Comparing Fig. 2-(b) to Fig. 2-(a), we can observe that there is a scale factor in the SBD error, which can be incorporated in the step-size of the SBD algorithm. Furthermore, since the envelope grows

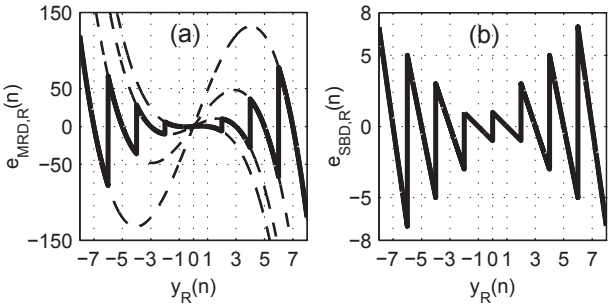

Fig. 2. Real part of the error for (a) MRD (64-QAM, solid curve) and MMA (4-QAM with different scale factors, dashed curves); (b) SBD (64-QAM).

linearly and not exponentially as in the MRD error, the performance of the SBD algorithm tends to be better than that of the MRD one.

The regional multimodulus algorithm (RMA) of [11] can be interpreted as a member of the proposed family of algorithms since its error is zero when the equalizer output is equal to one of the constellation symbols. This algorithm uses the error shown in Fig. 3, where is considered the real part of a 64-QAM constellation. The RMA error is obtained through the repetition of the MMA error shape for $r = 1$ in regions denoted by $A_{m,\rm R}$ with $m = -2, -1, 1, 2$, weighted by a scale factor[1]. The centers of the regions $A_{m,\rm R}$ are denoted by $c_{m,\rm R}$ and are indicated by circles in the figure. Each center $c_{m,\rm R}$ is equidistant from two adjacent symbol coordinates contained in the region $A_{m,\rm R}$ and indicated by asterisks. As in the MRD and SBD errors, scale factors had to be imposed to create an envelope in the error function and allow a proper recovery of the transmitted signals. These factors depend on the region as shown in the sequel.

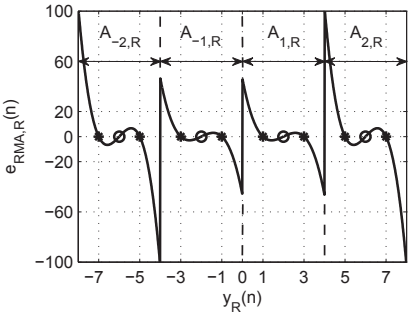

Fig. 3. Real part of the error of RMA as a function of $y_{\rm R}(n)$ for 64-QAM.

Given the equalizer output $y(n)$ and assuming a square S-QAM constellation, with $(\log_2(S) - 2)$ comparisons, it is possible to identify to which regions $A_{\ell,\rm R}$ and $A_{\ell,\rm I}$ the real and imaginary parts of the equalizer output belong. Using this information, an expression for the RMA error can be defined as

$$e_{\rm RMA}(n) = \alpha_{\ell,\rm R}\,\big[1 - \bar{y}_{\ell,\rm R}^2(n)\big]\,\bar{y}_{\ell,\rm R}(n) + j\alpha_{\ell,\rm I}\,\big[1 - \bar{y}_{\ell,\rm I}^2(n)\big]\,\bar{y}_{\ell,\rm I}(n), \quad (5)$$

where $\bar{y}_{\ell,\rm R}(n) = y_{\rm R}(n) - c_{\ell,\rm R}$ and $\bar{y}_{\ell,\rm I}(n) = y_{\rm I}(n) - c_{\ell,\rm I}$ are translated versions of the real and imaginary parts of the equalizer output, $c_{\ell,\rm R}$ and $c_{\ell,\rm I}$ are the centers of the identified regions, and $\alpha_{\ell,\rm R}$ and $\alpha_{\ell,\rm I}$ are scale factors, which depend on the region. Due to the shift of the estimates $y_{\rm R}(n)$ and $y_{\rm I}(n)$ to the origin, everything happens as if only the symbols $\{\pm 1 \pm j\}$ of a 4-QAM constellation had been transmitted. Therefore, given the regions $A_{\ell,\rm R}$ and $A_{\ell,\rm I}$ with symbols coordinates represented respectively by $a_{\ell,\rm R}$ and $a_{\ell,\rm I}$, RMA seeks to minimize the regional cost function

$$J_\ell = \mathrm{E}\left\{\alpha_{\ell,\rm R}\big[1 - \bar{y}_{\ell,\rm R}^2(n)\big]^2\right\} + \mathrm{E}\left\{\alpha_{\ell,\rm I}\big[1 - \bar{y}_{\ell,\rm I}^2(n)\big]^2\right\}.$$

[1]In the case of a square S-QAM, there are $\sqrt{S}/2$ regions $A_{m,\rm R}$, where $m = -\sqrt{S}/4, \cdots, -1, 1, \cdots, \sqrt{S}/4$ (similarly for the imaginary part).

Assuming $\sqrt{\alpha_{\ell,\mathrm{R}}}\ \bar{y}^2_{\ell,\mathrm{R}}(n) = \beta_{\mathrm{R}} a^2_{\ell,\mathrm{R}}(n)$ with β_{R} being a constant, and calculating $\partial J_{\ell,\mathrm{R}}/\partial\beta_{\mathrm{R}}|_{\beta_{\mathrm{R}}=1} = 0$, we obtain the optimal value of $\alpha_{\ell,\mathrm{R}}$, i.e., $\alpha_{\ell,\mathrm{R}} = [\mathrm{E}\{a^4_{\ell,\mathrm{R}}(n)\}/\mathrm{E}\{a^2_{\ell,\mathrm{R}}(n)\}]^2$. Similarly for the imaginary part, $\alpha_{\ell,\mathrm{I}} = [\mathrm{E}\{a^4_{\ell,\mathrm{I}}(n)\}/\mathrm{E}\{a^2_{\ell,\mathrm{I}}(n)\}]^2$. Considering 64-QAM, for example, we obtain $\alpha_{-1,\mathrm{R}} = \alpha_{1,\mathrm{R}} = 2.86^2$ and $\alpha_{-2,\mathrm{R}} = \alpha_{2,\mathrm{R}} = 6.39^2$. We can observe that the farther the region $A_{\ell,\mathrm{R}}$ is from the origin, the closer the value of $\alpha_{\ell,\mathrm{R}}$ is to the square of the center of the region $c^2_{\ell,\mathrm{R}}$.

The proposed family of algorithms present two main drawbacks: (i) it still has the typical slow convergence of MMA and (ii) the algorithms can diverge in some situations. We address these two issues in the next section.

4. ON THE CONVERGENCE AND THE STABILITY

At the initial iterations, the coefficient vector $\mathbf{w}$ can be very distant from the optimal solution, and the equalizer output can fall in a wrong region, mainly in the presence of noise. This wrong decision is fed back and the algorithm can take many iterations to converge.

To improve the convergence of the presented family of algorithms, we can use the philosophy proposed in [11] for RMA. Assuming that the real part of the equalizer output falls in the region $A_{\ell,\mathrm{R}}$, the error should take into account not only the region $A_{\ell,\mathrm{R}}$, but also the regions $A_{\ell-1,\mathrm{R}}$ and $A_{\ell+1,\mathrm{R}}$ in its neighborhood (similarly for the imaginary counterpart). Note that if $A_{\ell,\mathrm{R}}$ is a region of the constellation edges, there will be only inner neighbors. Fig. 4-(a) shows the regions of the real part of a 64-QAM constellation, assuming that $y_{\mathrm{R}}(n)$ is in $A_{-1,\mathrm{R}}$. The real part of the RMA error can be calculated as

$$e_{\mathrm{RMA,R}}(n) = \sum_{m=\ell-1}^{\ell+1} \gamma_{m,\mathrm{R}}\alpha_{m,\mathrm{R}}\left[1-\bar{y}^2_{m,\mathrm{R}}(n)\right]\bar{y}_{m,\mathrm{R}}(n),$$

where $\gamma_{m,\mathrm{R}} = 1$ for $m = \ell$ (main region) and $\gamma_{m,\mathrm{R}} = 1/16$ for $m = \ell \pm 1$ (regions in the neighborhood). These values were experimentally chosen in [11] and are important to impose a distinction among the errors calculated in the neighborhood and that of the main region, i.e., the farther the neighbor, the smaller the weight $\gamma_{\ell,\mathrm{R}}$. Depending on the order of the QAM constellation, more than two regions can be considered in the neighborhood of the main region of each real and imaginary part of the equalizer output. However, we observed through simulations from 64 to 1024-QAM that two neighbors for the real part and two for the imaginary part are sufficient to improve significantly the convergence of RMA.

Using a similar idea for the MRD and SBD algorithms, we can speed up their convergences. The main difference from RMA is that the regions are now constituted only by one symbol coordinate. Fig. 4-(b) shows the regions of the real part of a 64-QAM constellation, assuming again that $y_{\mathrm{R}}(n)$ is in $A_{-1,\mathrm{R}}$. Let $a_{m,\mathrm{R}}$ be the real coordinate of the constellation symbol at the region $A_{m,\mathrm{R}}$, the real part of the MRD and SBD errors can be computed respectively as

$$e_{\mathrm{MRD,R}}(n) = \sum_{\substack{m=\ell-1\\ \ell+1}}^{\ell+1} \gamma_{m,\mathrm{R}}\left[a^2_{m,\mathrm{R}} - y^2_{\mathrm{R}}(n)\right]y_{\mathrm{R}}(n), \text{ and} \qquad (6)$$

$$e_{\mathrm{SBD,R}}(n) = \sum_{m=\ell-1}^{\ell+1} \gamma_{m,\mathrm{R}}|a_{m,\mathrm{R}}|\left[a_{m,\mathrm{R}} - y_{\mathrm{R}}(n)\right]. \qquad (7)$$

For both cases, $\gamma_{m,\mathrm{R}} = 1$ for $m = \ell$ and $\gamma_{m,\mathrm{R}} = 1/4$ for $m = \ell \pm 1$.

The convergence rate of the proposed algorithms can be improved with the aid of the neighbors. However, their steady-state mean-square decision errors (MSE) can increase due to the neighbor errors summed to the main error at each time instant. Thus, the aid of the neighbors should be disregarded when the algorithms achieve the steady-state. For this purpose, instead of weighting the neighbor errors by d^{-2}, where $d = 4$ for RMA and $d = 2$ for MRD and SBD, we consider a time function $\gamma_{m,\mathrm{R}}(n) = d^{-p(n)}$, where

$$p(n) = 7.1467\frac{1-\mathrm{e}^{8[\xi(n)-0.03]}}{1+\mathrm{e}^{8[\xi(n)-0.03]}} + 9.1467,$$

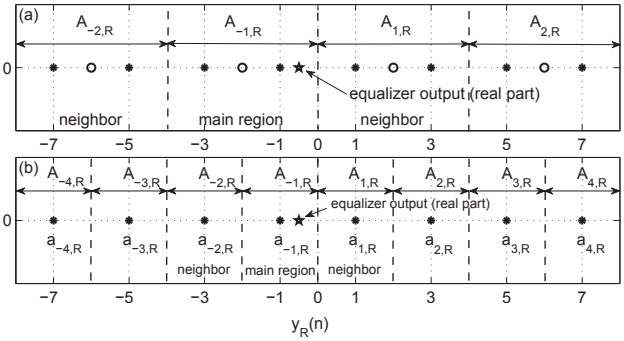

Fig. 4. Regions of the real part of 64-QAM for (a) RMA; (b) MRD and SBD.

and $\xi(n) = \lambda\xi(n-1) + (1-\lambda)|e_d(n)|^2$ is an estimate of the mean-squared decision error, being $e_d(n) = \hat{a}(n) - y(n)$ and $0 \ll \lambda < 1$ a forgetting factor. It should be notice that $2 \le p(n) \le 10$ and that the smaller the MSE, the larger is the value of $p(n)$, and consequently the smaller the weight $\gamma_{m,\mathrm{R}}(n)$. This function was experimentally chosen in [11] for RMA and is extended here for the MRD and SBD algorithms. Through simulations, we observe that $p(n)$ is important to make the MSE of the algorithms smaller at the steady-state.

To obtain a sufficient condition for the exponential stability of the normalized version of the SBD algorithm without considering the neighbors, we particularize its error by replacing the factors $|\hat{a}_{\mathrm{R}}(n)|$ and $|\hat{a}_{\mathrm{I}}(n)|$ by $\max\left\{|\hat{a}_{\mathrm{R}}(n)|, |\hat{a}_{\mathrm{I}}(n)|\right\}$, which leads to

$$e_{\mathrm{SBD}}(n) = \max\left\{|\hat{a}_{\mathrm{R}}(n)|, |\hat{a}_{\mathrm{I}}(n)|\right\}\left[\hat{a}(n) - y(n)\right]. \qquad (8)$$

Using (8) in conjunction with (deterministic) exponential stability results for the normalized least mean-square algorithm (see, e.g., [12, p. 78]), we conclude that the SBD algorithm is stable if the step-size $\tilde{\mu}$ is chosen in the interval

$$0 < \tilde{\mu} < 2/B \le 2/\max\left\{|\hat{a}_{\mathrm{R}}(n)|, |\hat{a}_{\mathrm{I}}(n)|\right\},$$

where B is the maximum absolute value of the coordinate of the constellation symbol. Assuming now that $y_{\mathrm{R}}(n)$ and $y_{\mathrm{I}}(n)$ fall respectively in $A_{\ell,\mathrm{R}}$ and $A_{m,\mathrm{I}}$ with neighbors $A_{\ell\pm1,\mathrm{R}}$ and $A_{m\pm1,\mathrm{I}}$, and using the symmetry properties $\hat{a}_{\ell\pm1,\mathrm{R}} = \hat{a}_{\ell,\mathrm{R}} \pm 2$ and $\hat{a}_{m\pm1,\mathrm{I}} = \hat{a}_{m,\mathrm{I}} \pm 2$, we can show that the stability of the SBD algorithm is ensured if

$$0 < \tilde{\mu} < 2/[B(1+2\gamma_{\max})],$$

where $\gamma_{\max}$ is the maximum value of $\{\gamma_{\ell\pm1,\mathrm{R}}(n), \gamma_{m\pm1,\mathrm{I}}(n)\}$. For $\gamma_{\max} = 1/4$, this interval reduces to $0 < \tilde{\mu} < 1.334B^{-1}$.

Since RMA and the MRD algorithm are based on MMA, they can converge to local minima or even diverge when the step-size is not properly chosen or if the initialization is distant from the optimal solution [13]. In order to avoid divergence, a dual-mode CMA was proposed in [13]. In the first mode, this algorithm works as the normalized CMA, while in the second mode, it rejects non-consistent estimates of the transmitted signal. In [11], this philosophy was used in RMA, which uses $\alpha_{\ell,\mathrm{R}}$ and $\alpha_{\ell,\mathrm{I}}$ equal to the absolute values of the centers of the regions. Although we do not provide a proof of convergence yet, the dual-mode RMA seems to be stable if $0 < \tilde{\mu} < 4/|c_{\max}|$ or if $0 < \tilde{\mu} < 3.2/|c_{\max}|$ considering the neighbors, where $|c_{\max}|$ is the absolute value of the center of the farthest region from the origin. This philosophy can also be used to avoid divergence in the MRD algorithm.

5. SIMULATION RESULTS AND CONCLUSION

The equalizers were initialized with the typical center spike and we used the normalized versions of all algorithms with $\delta = 10^{-8}$ in all simulations. Instead of using the optimum values of $\alpha_{\ell,\mathrm{R}}$ and $\alpha_{\ell,\mathrm{I}}$ in RMA, we used the absolute values of the centers of the regions. This facilitates its implementation since the distance between centers of adjacent regions is always equal to 4.

Fig. 5 shows the mean-squared decision error (MSE) estimated from the ensemble-average of 100 independent runs for 64-QAM (Fig. 5-a) and 1024-QAM (Fig. 5-b). We assume a fractionally-spaced equalizer with $M = 10$ coefficients and the channel $\mathbf{h}^T = [-0.2+j0.3 \;\; -0.5+j0.4 \;\; 0.7-j0.6 \;\; 0.4+j0.3 \;\; 0.2+j0.1 \;\; -0.1+j0.2]$ in the absence of noise. For both constellations, MMA presents a high misadjustment due to nonconstant modulus signals. On the other hand, RMA and SBD outperform MMA, converging to the Wiener solution, which provides perfect equalization in this case (-300 dB in the Matlab precision). MRD has shown good performance only for constellations up to 64-QAM. For high-order QAM, it fails to converge as we can observe comparing Fig. 5-a to Fig. 5-b.

To illustrate the influence of the neighbors, Fig. 6 shows the MSE for RMA and SBD with neighbors (solid curves) and without neighbors (dotted curves), considering the voice-band telephonic channel used in [8], absence of noise, 21 taps, 1024-QAM (Fig. 6-a), and 4096-QAM (Fig. 6-c). For both constellations, SBD and RMA converge to the Winner solution and the neighbors largely improve their convergence rates. Figs. 6-b and 6-d show the ensemble-average of the exponent $p(n)$. When $p(n) \approx 10$, the aid of the neighbors could be disregarded for RMA and SBD without performance degradation. Note that for 1024-QAM, only two neighbors for the real part and two for the imaginary part were used. However, we used four neighbors for the real part and four for the imaginary part in the 4096-QAM case, since less neighbors are not sufficient to speed up their convergences. It is important to notice that sometimes the proposed algorithms does not converge to the best Wiener solution. However, this issue can be solved by adjusting the initialization of the algorithms.

Fig. 7 shows curves of symbol error rate (SER) as a function of the signal-to-noise ratio (SNR), assuming the same scenario of the previous simulation. The curve for an AWGN channel is considered as a benchmark and indicated by OPT. For 1024-QAM (Fig. 7-a), RMA performs close to SBD and both outperform MMA, whose SER tends to 10^{-3}. Similar performance can be observed for 4096-QAM, but in this case MMA leads to an SER of 10^{-1}.

Fig. 8 shows the squared decision error for a time-variant channel in the absence of noise and 1024-QAM. We assume the same voice-band channel of [8], but replace its last coefficient by $0.2\sin(2 \times 10^{-6}\pi n)$. RMA and SBD track the channel variation, presenting $e_d^2(n)$ at least 10 dB lower than that of MMA, which does not converge. In this case, RMA converges faster than the SBD algorithm.

To the best of our knowledged, the literature does not contain algorithms that perform similarly to RMA and SBD for high-order QAM signals. The simulation results suggest that these algorithms can be used in practical situations, where the blind equalization of high-order QAM signals is required. In a future work, we intend to extend the stability analysis and provide a statistical analysis to confirm theoretically the good behavior of RMA and SBD.

6. REFERENCES

[1] R. L. Howald, "QAM bulks up once again: Modulation to the power of ten," in *Proceedings of SCTE Cable-tec EXPO*, Jun. 2002. Avaiable at http://broadband.motorola.com/ips/pdf/QAM.pdf.

[2] J.-T. Yuan and T.-C. Lin, "Equalization and carrier phase recovery of CMA and MMA in blind adaptive receivers," *IEEE Trans. Signal Process.*, vol. 58, pp. 3206–3217, Jun. 2010.

[3] M. T. M. Silva and V. H. Nascimento, "Tracking analysis of the Constant Modulus Algorithm," in *Proc. of ICASSP*, 2008, pp. 3561–3564.

[4] J. Yang, J.-J. Werner, and G. A. Dumont, "The multimodulus blind equalization and its generalized algorithms," *IEEE J. Sel. Areas Commun.*, vol. 20, pp. 997–1015, Jun. 2002.

[5] J.-T. Yuan and K.-D. Tsai, "Analysis of the multimodulus blind equalization algorithm in QAM communication systems," *IEEE Trans. Commun.*, vol. 53, pp. 1427–1431, Sep. 2005.

[6] M. J. Ready and R. P. Gooch, "Blind equalization based on radius directed adaptation," in *Proc. of ICASSP*, 1990, vol. 3, pp. 1699–1702.

[7] A. Labed et al., "New hybrid adaptive blind equalization algorithms for QAM signals," in *Proc. of ICASSP*, 2009, pp. 2809–2812.

[8] S. Abrar and A.K. Nandi, "Blind equalization of square-QAM signals," *IEEE Trans. Commun.*, vol. 58, pp. 1674–1685, Jun. 2010.

[9] A. H. Sayed, *Adaptve Filters*, John Wiley & Sons, NJ, 2008.

[10] K. N. Oh and J. H. Park, "Property restoral approach to blind equalization of digital transmission channels," *IEEE Trans. Consum. Electron.*, vol. 43, pp. 544–549, Aug. 1997.

[11] J. Mendes Filho, M. T. M. Silva, M. D. Miranda, and V. H. Nascimento, "A region-based algorithm for blind equalization of QAM signals," in *Proc. of IEEE Workshop on Statist. Signal Process.*, 2009, pp. 685–688.

[12] I. Mareels and J. W. Polderman, *Adaptive systems: an introduction*, Birkhäuser, Boston, 1996.

[13] M. D. Miranda, M. T. M. Silva, and V. H. Nascimento, "Avoiding divergence in CMA," in *Proc. of ICASSP*, 2008, pp. 3565–3568.

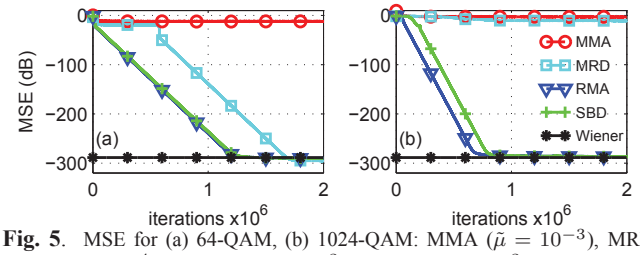

Fig. 5. MSE for (a) 64-QAM, (b) 1024-QAM: MMA ($\tilde{\mu} = 10^{-3}$), MRD ($\tilde{\mu} = 1.75 \times 10^{-4}$), RMA ($\tilde{\mu} = 5 \times 10^{-3}$), SBD ($\tilde{\mu} = 5 \times 10^{-3}$), no neighbors.

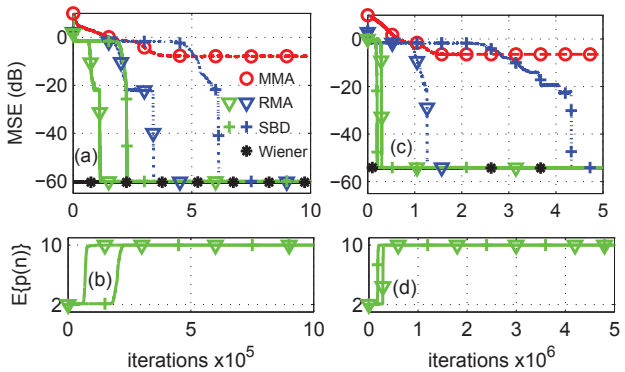

Fig. 6. MSE and E$\{p(n)\}$ for (a) and (b) 1024-QAM, RMA and SBD ($\tilde{\mu} = 5 \times 10^{-4}$), RMA and SBD with 4 neighbors ($\tilde{\mu} = 5 \times 10^{-3}$); (c) and (d) 4096-QAM, SBD, RMA, and RMA with 8 neighbors ($\tilde{\mu} = 2 \times 10^{-3}$), SBD with 8 neighbors ($\tilde{\mu} = 3 \times 10^{-3}$); MMA ($\tilde{\mu} = 10^{-3}$); $M = 21$; average of 100 runs.

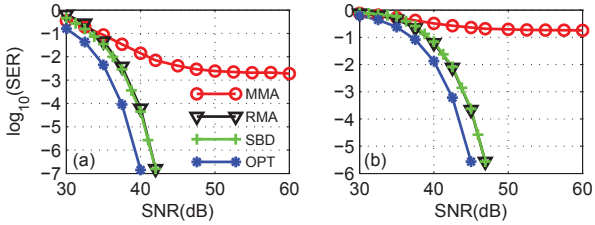

Fig. 7. Log of SER as a function of SNR for (a) 1024-QAM (b) 4096-QAM.

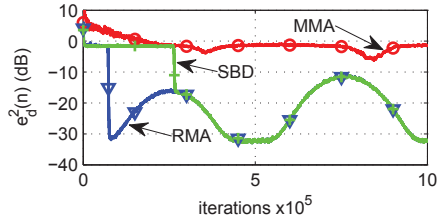

Fig. 8. Squared decision error for a time-variant channel, RMA and SBD ($\tilde{\mu} = 5 \times 10^{-3}$), MMA ($\tilde{\mu} = 10^{-3}$), $M = 21$.